Search for η-mesic Helium with WASA-at-COSY facility

Magdalena Skurzok
Jagiellonian University, Krakow, Poland

for WASA-at-COSY Collaboration

EMMI Workshop "Meson and Hyperon Interactions with Nuclei"
13-16.09.2022

Introduction – η-mesic bound state

η-mesic nucleus

^4He-η

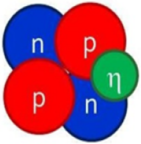

strong interaction

$$m_{bound} = m_{^4He} + m_\eta - B_s$$

meson 

$u\bar{u}$, $d\bar{d}$, $s\bar{s}$

$$\eta_1 = \frac{1}{\sqrt{3}}(d\bar{d} + u\bar{u} + s\bar{s}),$$
$$\eta_8 = \frac{1}{\sqrt{6}}(d\bar{d} + u\bar{u} - 2s\bar{s})$$

$|\eta> = \eta_8 cos\theta - \eta_1 sin\theta$, θ = -15.5°±1.3°

m_η=547.86 MeV
Γ=1.31 keV
$\tau=10^{-18}$ s
(PDG 2020)

main decay channels:

$\eta \to 2\gamma$	~39%
$\eta \to 3\pi^0$	~33%
$\eta \to \pi^0\pi^+\pi^-$	~23%

$|Re(a_{\eta N})| > Im(a_{\eta N})$

attraction > absorption

η interaction with nucleon

For low energies η-N interaction dominated by N^*

N^* resonance: $m_N^* \approx 1535\text{MeV}$ $\Gamma \approx 150\text{MeV}$ $J^P = \frac{1}{2}^-$

Main decay channels:

$N^* \rightarrow \pi N$ (35-55 %)

$N^* \rightarrow \eta N$ (30-55 %)

$N^* \rightarrow \pi\pi N$ (1-10 %)

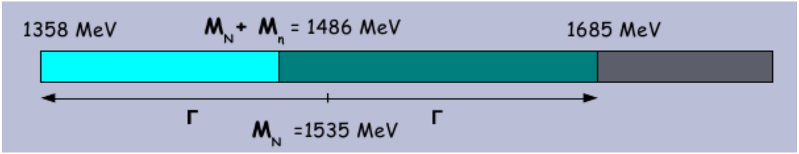

impossible to create the η beams $\Rightarrow$ η-N studies based on the investigation of ηN scattering amplitude for the processes like πN $\rightarrow$ ηN, γN $\rightarrow$ ηN $\Rightarrow$ N^* domination (coupled mainly to ηN and πN)

Coupled channel calculations $\Rightarrow$ fit to available experimental data

Attractive and strong interaction between η and nucleon

R. Bhalerao, L. C. Liu, Phys. Lett. B54, 685 (1985)

($a_{\eta N}$=0.28+i0.19 fm)

⇓

Possible existence of η-mesic bound states postulated for atomic nuclei with A>12

Q. Haider, L. C. Liu, Phys. Lett. B172, 257 (1986)

Recent theoretical studies of hadronic- and photoproduction of η meson support the existence of light η-mesic nuclei like $(^3\text{He-}\eta)_{bound}$ $(^4\text{He-}\eta)_{bound}$

$B_s \in (1, 40)$ MeV, $\Gamma \in (1, 45)$ MeV

0.18 fm<Re($a_{\eta N}$)<1.03fm
0.16 fm<Im($a_{\eta N}$)<0.49 fm

$dd \rightarrow (^4\text{He-}\eta)_{bound} \rightarrow {}^3\text{He}p\pi^-$: σ=**4.5 nb** | $pd \rightarrow (^3\text{He-}\eta)_{bound} \rightarrow Xp\pi^-$: σ=**80 nb**

J.-J. Xie et al., Eur. Phys. J. A 55 no.1, 6 (2019)
J.-J. Xie et al., Phys. Rev. C 95, 015202 (2017)
T. Ishikawa et al., Phys.Rev.C 105 (2022) 4, 045201
Phys.Rev.C 104 (2021) 5, L052201
M. Skurzok et al., Nucl. Phys. A 993, 121647 (2020)
N. Ikeno et al., Eur. Phys. J A 53 no. 10, 194 (2017)
T. Ishikawa et al., Acta. Phys. Polon. B 51, 27 (2020)
T. Sekihara, H. Fujioka, T. Ishikawa, Phys. Rev. C 97, 045202 (2017)
A. Fix and O. Kolesnikov, Phys. Rev. C 97, 044001 (2018)
V. Metag, M. Nanova, E. Paryev, Prog. Part. Nucl. Phys. 97, 199 (2017)
J. Mares et al., Acta. Phys. Polon. B 51, 129 (2020)
N. G. Kelkar, H. Kamada, M. Skurzok, Int. J. Mod. Phys. E 28, 1950066 (2019)
N. G. Kelkar, D. Bedoya Fierro, H. Kamada, M. Skurzok, Nucl. Phys. A 996, 121698 (2020)
S. D. Bass and P. Moskal, Rev.Mod. Phys. 91, 015003 (2019)
S. Wycech, W. Krzemien, Acta. Phys. Polon B 45, 745 (2014)
C. Wilkin, Acta. Phys. Polon. B 45, 603 (2014)

Exp. indications of the existence of the ^{3}He-η bound state

total cross section $pd \rightarrow$ ^{3}He-η $\frac{d\sigma(\theta_\eta)}{d\Omega} = \frac{\sigma_{tot}}{4\pi}(1 - \alpha cos\theta_\eta)$

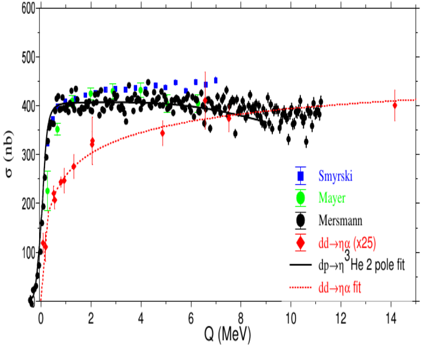

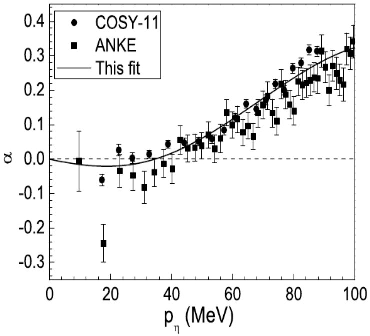

Strong *He*-η interaction

strong variation of the phase of s-wave production amplitude with energy

Exp. indications of the existence of the ^{3}He-η bound state

total cross section $\quad pd \rightarrow {}^3\text{He-}\eta \quad \frac{d\sigma(\theta_\eta)}{d\Omega} = \frac{\sigma_{tot}}{4\pi}(1 - \alpha cos\theta_\eta)$

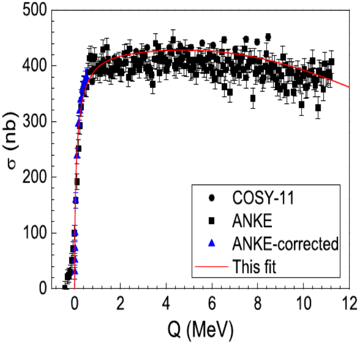

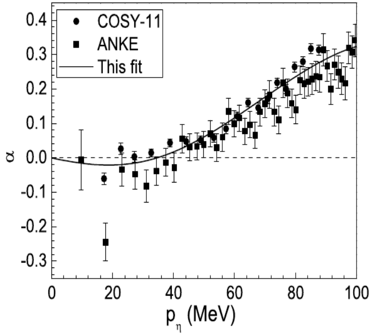

$\Downarrow$

J.-J. Xie, et al., Phys. Rev. C 95, 015202 (2017)

"weakly bound ^{3}*He-*η *state with* binding energy *of the order of* 0.3 MeV *and a* width *of the order of* 3 MeV*"*, $a_{\eta 3He} = [-(2.23 \pm 1.29) - i(4.89 \pm 0.57)]$ *fm*

COoler SYnchrotron COSY

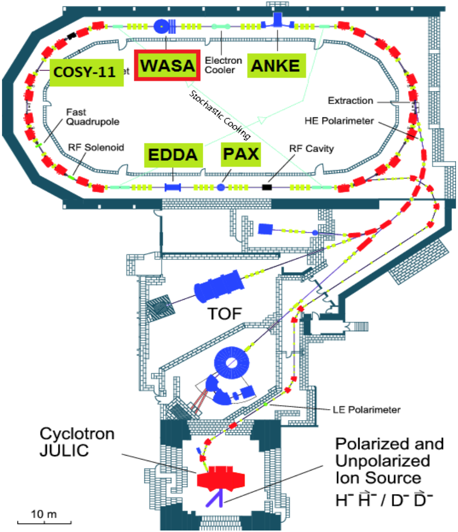

- 184 m circumference cooler synchrotron
- Polarized and unpolarized proton and deuteron beam
- Momentum range 0.3 - 3.7 GeV/c
- Stochastic and electron cooling
- 10^{11} particles in ring - luminosities 10^{31} - 10^{32} $cm^{-2}s^{-1}$
- Ramped beam (search for η-mesic nuclei)

WASA-at-COSY experiment

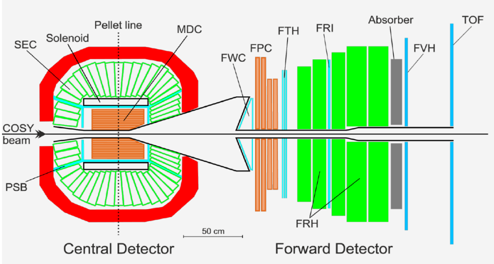

- **Pellet Target**
  - frozen pellets of hydrogen or deuterium

- **Forward Detector**
  - identification of heavier projectiles and target-recoil particles such as p, d and He in forward direction
  - angular information about the particles provided by FPC
  - PID based on measurement of energy loss in scintillators

- **Central Detector**
  - charged particles momenta reconstructed in magnetic field (MDC)
  - PID based on measurement of energy loss in scintillators
  - photons identified in calorimeter

Status of the search for η-mesic Helium at WASA

$(^4\text{He-}\eta)_{bound}$

- **2008**: $dd \rightarrow {}^3\text{He}p\pi^-$ reaction

  P. Adlarson et al., Phys. Rev. C87, 035204 (2013)

- **2010**: $dd \rightarrow {}^3\text{He}n\pi^0$ and $dd \rightarrow {}^3\text{He}p\pi^-$ reactions

  P. Adlarson et al., Nucl. Phys. A 959, 102-115 (2017)

  M. Skurzok, P. Moskal, et al., Phys. Lett. B782, 6-12 (2018)

$\Uparrow$

η meson absorption and excitation of one of the nucleons to an N^* resonance, which subsequently decays into an N - π pair

$(^3\text{He-}\eta)_{bound}$

- **2014**:

  - $pd \rightarrow {}^3\text{He}2\gamma({}^3\text{He}6\gamma)$ reactions

  P. Adlarson et al., Phys. Lett. B 802, 135205 (2020)

  decay of the η - meson while it is still "orbiting" around a nucleus

  - $pd \rightarrow ppp\pi^-(ppn\pi^0, dp\pi^0)$ reactions

  P. Adlarson et al., Phys. Rev. C 102, 044322 (2020)

η meson absorption and excitation of one of the nucleons to an N^* resonance, which subsequently decays into an N - π pair

Papers available at http://koza.if.uj.edu.pl/publications/wasa-at-cosy

Experimental method

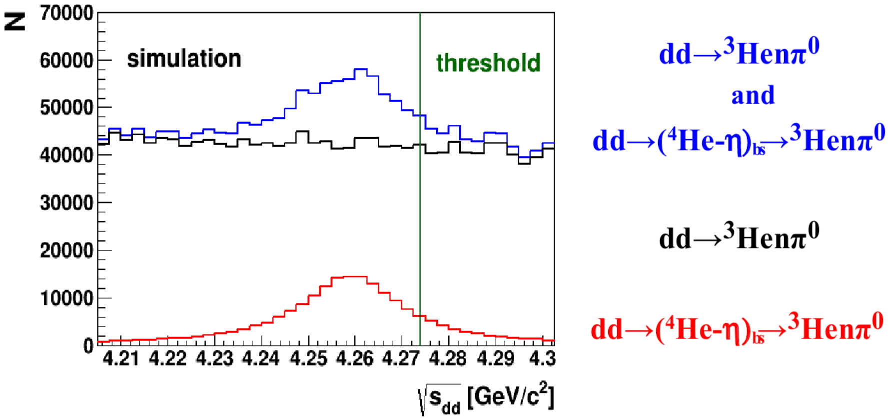

Excitation function

(^{4}**He**-η)$_{bound}$ **existence manifested by resonant-like structure below η production threshold**

Search for $(^4\text{He-}\eta)_{bound}$ with WASA-at-COSY

Exp. 186.1 & 186.2, FZ Jülich, Germany, 2008 and 2010

P. Moskal, W. Krzemien, J. Smyrski,
COSY proposal No. 186.1 & 186.2

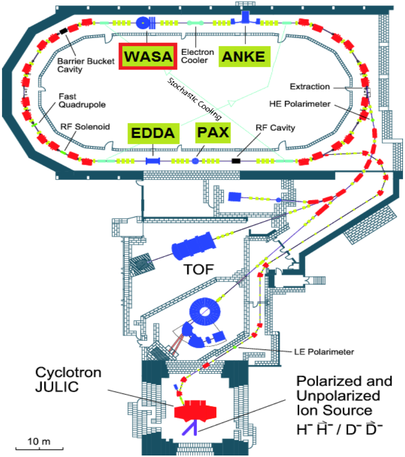

$dd \rightarrow {}^3\mathbf{He}n\pi^0$ | $dd \rightarrow {}^3\mathbf{He}p\pi^-$

- **Measurement** with the **deuteron** beam momentum ramped and with the **deuteron** pellet target

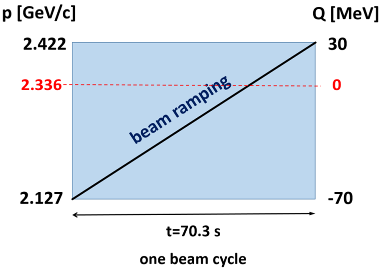

- **Data** were effectively taken with high acceptance (58%)

Search for $(^3\text{He-}\eta)_{bound}$ with WASA-at-COSY

Exp. 186.3, FZ Jülich, Germany 2014

P. Moskal, W. Krzemien, M. Skurzok, *COSY proposal No. 186.3*

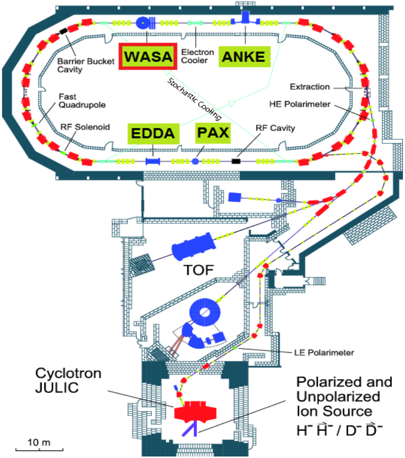

$pd \rightarrow ppp\pi^-(ppn\pi^0, dp\pi^0)$

$pd \rightarrow {}^3\mathbf{He}2\gamma\ ({}^3\mathbf{He}6\gamma)$

- **Measurement** with the **proton** beam momentum ramped and with the **deuteron** pellet target

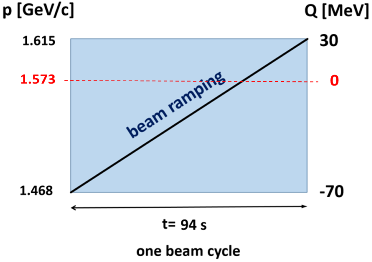

- **Data** were effectively taken with high acceptance

Kinematical mechanism of the reaction (via N^*)

$$dd \rightarrow (^4\text{He-}\eta)_{bs} \rightarrow {}^3\text{He}p\pi^-$$

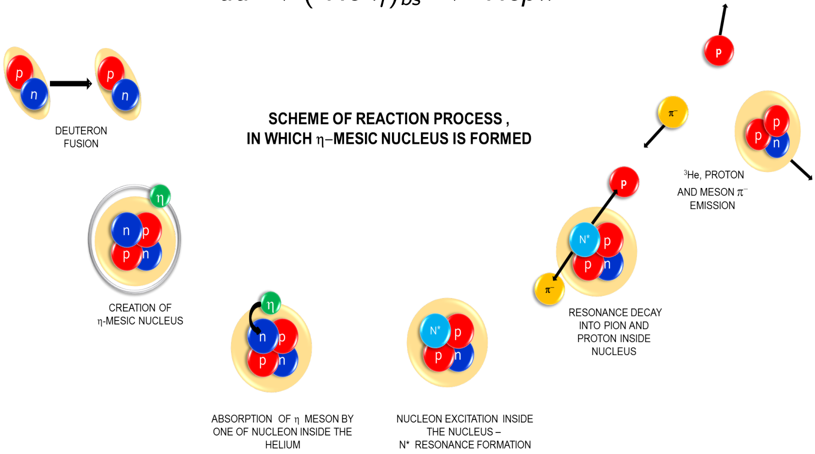

Kinematical mechanism of the reaction (via N^*)

$$dd \rightarrow (^4\text{He-}\eta)_{bs} \rightarrow {}^3\text{He}n\pi^0$$

SCHEME OF REACTION PROCESS , IN WHICH η–MESIC NUCLEUS IS FORMED

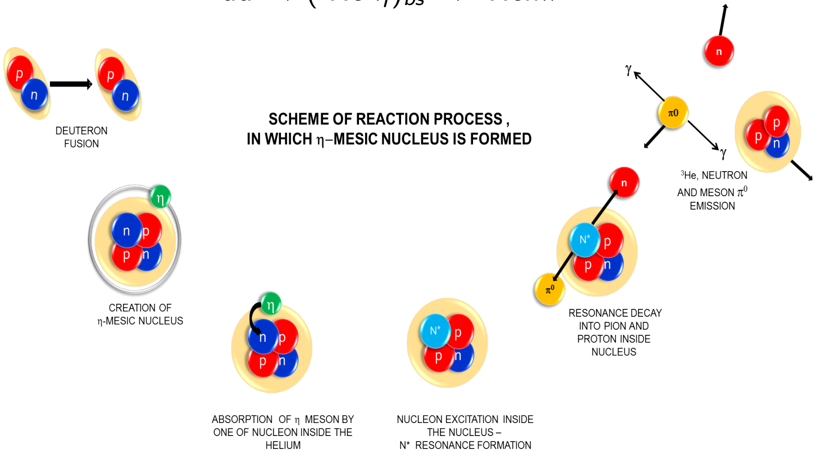

Simulation of $(^4\text{He-}\eta)_{bound}$ production and decay

Breit-Wigner distribution

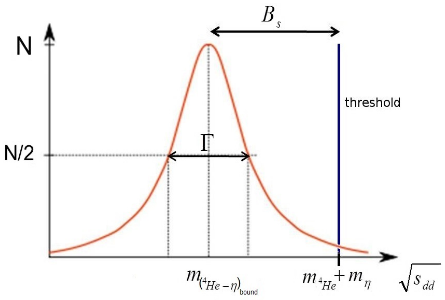

Spectator Model

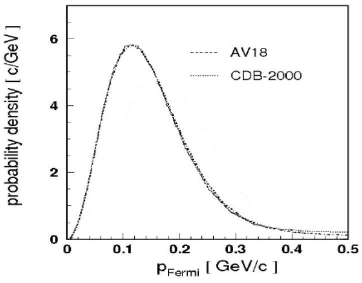

$$N\left(\sqrt{s_{dd}}\right) = \frac{1}{2\pi}\frac{\Gamma^2/4}{\left(\sqrt{s_{dd}}-m_{(^4He-\eta)_{bound}}\right)^2+\Gamma^2/4}$$

$$\left|\mathbb{P}_{^3He}\right|^2 = m^2_{^3He}$$

$$m_{(^4He-\eta)_{bound}} = m_{^4He} + m_\eta - B_s$$

Simulation of $(^4\text{He-}\eta)_{bound}$ production and decay

$$\eta + N \Rightarrow N^*(1535) \Rightarrow N + \pi = \begin{cases} p + \pi^- \\ n + \pi^0 \end{cases}$$

- relative N-π angle in the CM: $\theta_{cm}^{N,\pi} \sim 180^\circ$
- low ^{3}He momentum in the CM

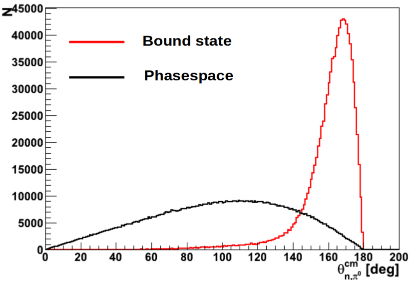

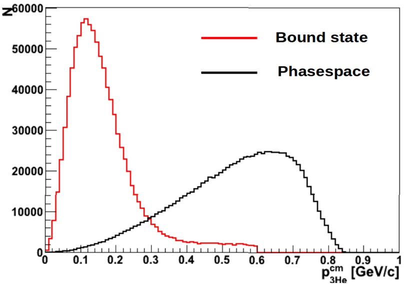

Experiment-May 2008

- **Channel:** $dd \rightarrow (^4\text{He-}\eta)_{bound} \rightarrow {}^3\text{He}p\pi^-$ (norm: $dd \rightarrow {}^3\text{He}n$)
- **Measurement:** beam momentum ramped from **2.185GeV/c to 2.400GeV/c** $\Rightarrow$ the range of excess energy **Q∈(-51,22)MeV**
- **Luminosity:** $L=118\frac{1}{nb}$
- **Acceptance:** A=53%

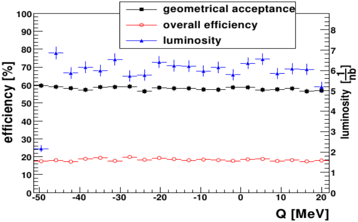

Excitation function

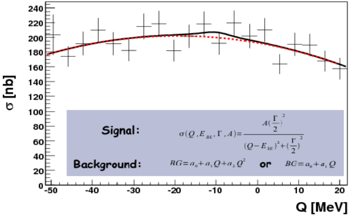

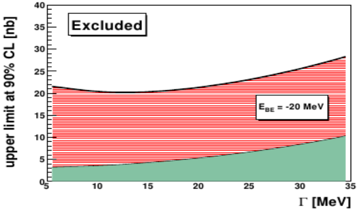

P. Adlarson et al., Phys. Rev. C87 (2013), 035204
W. Krzemien, Ph. D Thesis, Jagiellonian University (2012)

RESULT: $\sigma_{dd\rightarrow(^4He-\eta)_{bound}\rightarrow{}^3Hep\pi^-} < 27\ nb$

Experiment-Nov/Dec 2010

- **Channels:** $dd \rightarrow (^4\text{He-}\eta)_{bound} \rightarrow {}^3\text{He}p\pi^-$
  $dd \rightarrow (^4\text{He-}\eta)_{bound} \rightarrow {}^3\text{He}n\pi^0$
  (norm: $dd \rightarrow {}^3\text{He}n$ and $dd \rightarrow ppn_{sp}n_{sp}$)
- **Measurement:** beam momentum ramped from **2.127GeV/c to 2.422GeV/c** $\Rightarrow$ the range of excess energy **Q∈(-70,30)MeV**
- **Luminosity:** $L=1200\frac{1}{nb}$
- **Acceptance:** A=53%

⇓

about 10 times higher statistics than in 2008

ANALYSIS:

- Particles identification
- Selection bound state region
- Determination of excitation functions
- Determination the upper limit of the total cross section

Search for $(^4\text{He-}\eta)_{bound}$ in $dd \rightarrow {}^3\text{He}N\pi$ reaction | PID

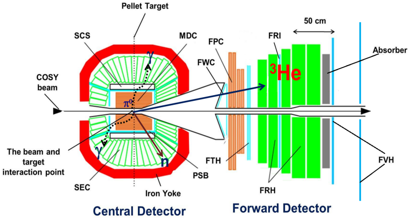

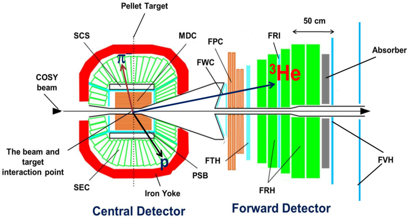

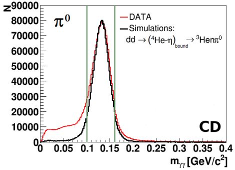

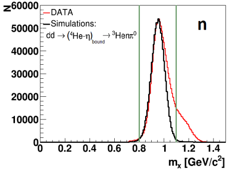

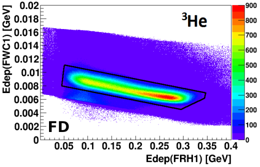

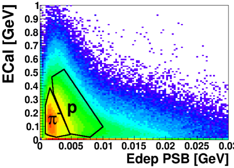

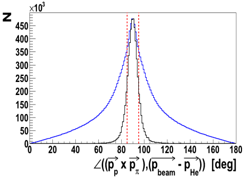

Search for $(^4\text{He-}\eta)_{bound}$ | Selection criteria

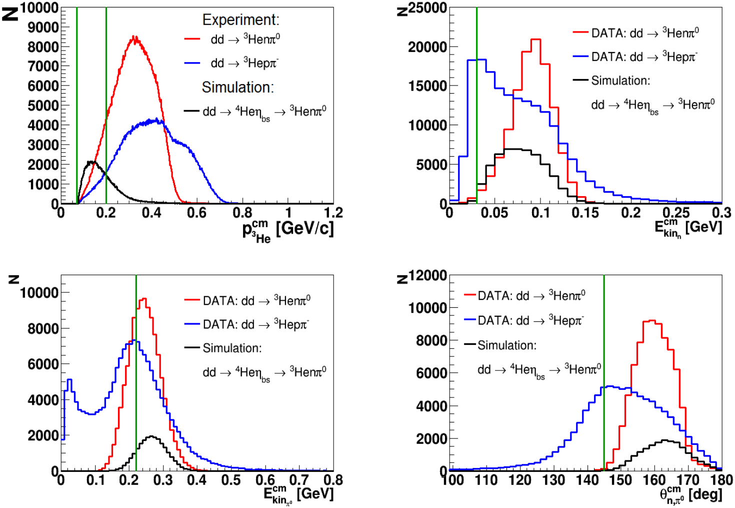

DATA: $dd \rightarrow {}^3\text{He}p\pi^-$

DATA: $dd \rightarrow {}^3\text{He}n\pi^0 \rightarrow {}^3\text{He}n\gamma\gamma$

Signal: $dd \rightarrow (^4\text{He-}\eta)_{bound} \rightarrow {}^3\text{He}n\pi^0$

Determination of the excitation function

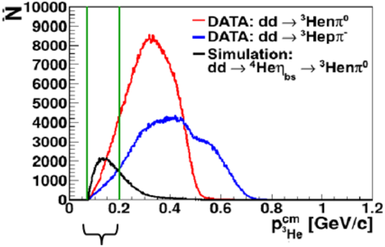

region rich in signal

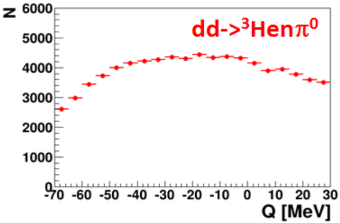

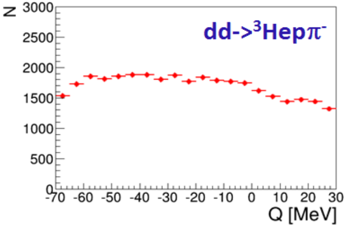

Determination of the total cross section for $dd \to {}^3\mathrm{He}n\pi^0$ reaction

Cross section

$$\sigma(Q) = \frac{N(Q)}{L(Q)\epsilon(Q)}$$

N - number of experimental events

L - integrated luminosity

ϵ - full detection efficiency

Excitation function

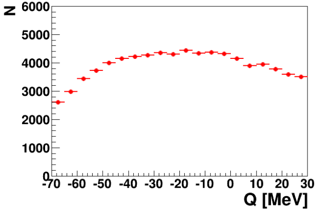

Efficiency

$dd \to ({}^4\mathrm{He}\text{-}\eta)_{bound} \to {}^3\mathrm{He}n\pi^0$

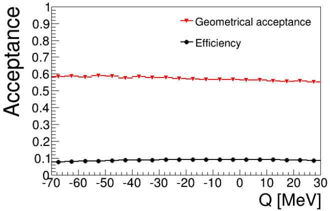

from simulations: $\epsilon = \frac{N_{acc}}{N_{gen}}$

Integrated luminosity

$dd \to ppn_{sp}n_{sp}$

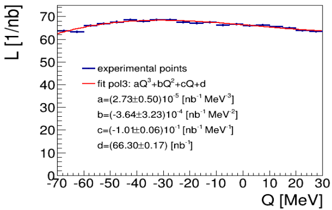

$dd \to ppn_{sp}n_{sp}$: $L = (1329 \pm 2_{stat} \pm 108_{syst} \pm 64_{norm})\,nb^{-1}$

$dd \to {}^3\mathrm{He}n$: $L = (1102 \pm 2_{stat} \pm 28_{syst} \pm 107_{norm})\,nb^{-1}$

Determination of the total cross section for $dd \rightarrow {}^3\mathrm{He}p\pi^-$ reaction

Cross section

$$\sigma(Q) = \frac{N(Q)}{L(Q)\epsilon(Q)}$$

N - number of experimental events

L - integrated luminosity

ϵ - full detection efficiency

Excitation function

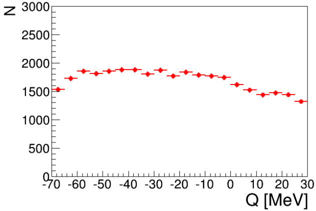

Efficiency

$dd \rightarrow ({}^4\mathrm{He}\text{-}\eta)_{bound} \rightarrow {}^3\mathrm{He}n\pi^0$

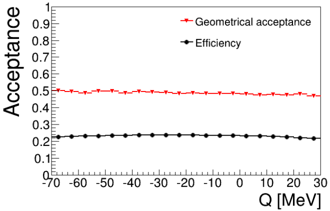

from simulations: $\epsilon = \frac{N_{acc}}{N_{gen}}$

Integrated luminosity

$dd \rightarrow ppn_{sp}n_{sp}$

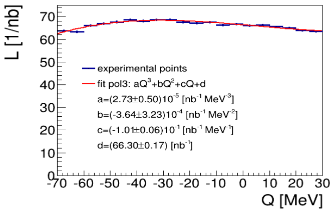

$dd \rightarrow ppn_{sp}n_{sp}$: $L = (1329 \pm 2_{stat} \pm 108_{syst} \pm 64_{norm})nb^{-1}$

$dd \rightarrow {}^3\mathrm{He}n$: $L = (1102 \pm 2_{stat} \pm 28_{syst} \pm 107_{norm})nb^{-1}$

Determination of the upper limit of the total cross section for $dd \to (^4\text{He-}\eta)_{bound} \to {}^3\text{He}N\pi$ processes at CL=90%

$dd \to (^4\text{He-}\eta)_{bound} \to {}^3\text{He}n\pi^0$

$\Downarrow$

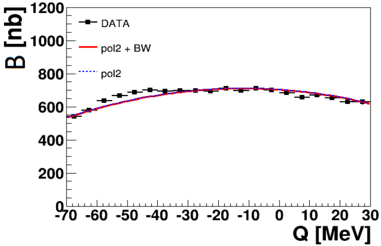

$dd \to (^4\text{He-}\eta)_{bound} \to {}^3\text{He}p\pi^-$

$\Downarrow$

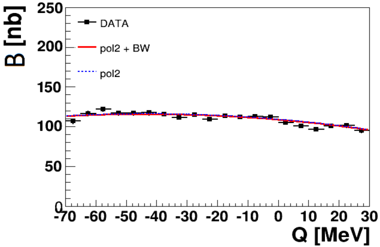

simultaneous fit with $\frac{A \cdot \Gamma^2/4}{(Q-B_s)^2+\Gamma^2/4} + BQ^2 + CQ + D$

Breit-Wigner (signal) + pol2 (background)

taking into account the **isospin relation** between the both of the considered channels:

$$P(N^* \to p\pi^-) = 2P(N^* \to n\pi^0)$$

B_s,Γ - fixed parameters | A, B, C, D - free parameters || $\sigma^{upp}_{CL=90\%} = k \cdot \sigma_A$, k=1.64 (for CL=90%)

Determination of the upper limit of the total cross section for $dd \rightarrow (^4He\text{-}\eta)_{bound} \rightarrow {}^3He p \pi^-$ process at CL=90%

$\sigma^{upp}_{CL=90\%}$ for
$dd \rightarrow (^4He\text{-}\eta)_{bound} \rightarrow {}^3He n \pi^0$
$\Downarrow$

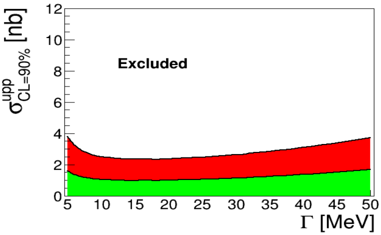

$\sigma^{upp}_{CL=90\%}$ for
$dd \rightarrow (^4He\text{-}\eta)_{bound} \rightarrow {}^3He p \pi^-$
$\Downarrow$

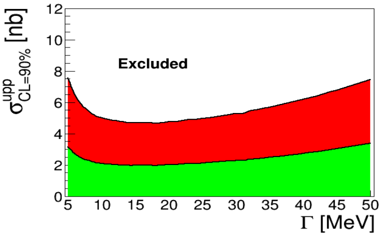

RESULT:
$\sigma_{dd \rightarrow (^4He-\eta)_{bound} \rightarrow {}^3He n \pi^0} < 3.5\ nb$

RESULT:
$\sigma_{dd \rightarrow (^4He-\eta)_{bound} \rightarrow {}^3He p \pi^-} < 7\ nb$
2008: $\sigma < 27\ nb$

P. Adlarson et al., Nucl. Phys. A 959, 102-115 (2017)

Systematics

Main contribution: momentum distribution for N^* inside He

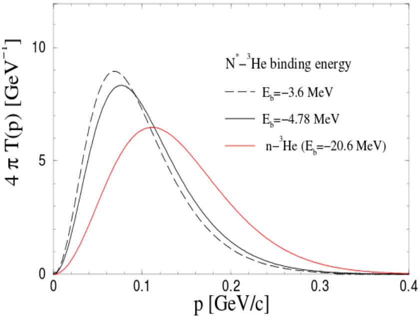

assumption that N^* resonance has a momentum distribution identical to the distribution of nucleons inside He

N^*-^3He momentum distribution determined: the elementary $NN^* \to NN^*$ interaction constructed within π and η meson exchange model $\Rightarrow$ N^*-He potential evaluated by folding NN^* interaction with a nuclear density

$\Downarrow$

Details:

N. G. Kelkar, Eur. Phys. J. A 52, 309 (2016)
N. G. Kelkar, D. Bedoya Ferro, P. Moskal, Acta Phys. Pol. B 47, 299 (2016)

Comparison with N. Ikeno et al. model prediction

N. Ikeno, H. Nagahiro, D. Jido, S. Hirenzaki, Eur. Phys. J. A 53, 194 (2017)

- total cross sections for the $dd \rightarrow (^4\text{He-}\eta)_{bound} \rightarrow {}^3\text{He}N\pi$ reaction determined based on phenomenological calculations
- the model reproduced the data on the $dd \rightarrow {}^4\text{He}\,\eta$ reaction quite well
- $\sigma = \sigma_{conv} + \sigma_{esc}$
- σ_{conv} - determined for different parameters V_0 and W_0 of a spherical η-^{4}He optical potential $V(r) = (V_0 + iW_0)\frac{\rho_\alpha(r)}{\rho_\alpha(0)}$ (the total cross section in the subthreshold excess energy region where the η meson is absorbed by the nucleus)
- normalization in the sense that the escape part reproduces the measured cross sections for the $dd \rightarrow {}^4\text{He}\eta$ process

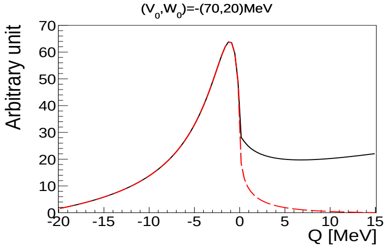

σ —

σ_{conv} - -

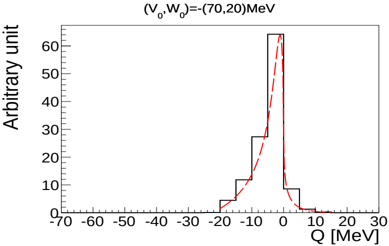

σ_{conv} spectrum convoluted with the experimental resolution functions

Comparison with N. Ikeno et al. model prediction

$dd \rightarrow (^4\text{He-}\eta)_{bound} \rightarrow {}^3\text{He}n\pi^0$ $\Downarrow$

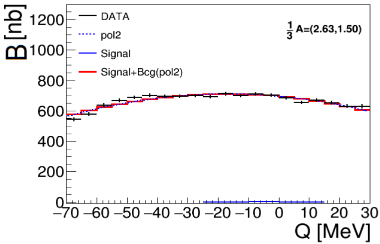

$dd \rightarrow (^4\text{He-}\eta)_{bound} \rightarrow {}^3\text{He}p\pi^-$ $\Downarrow$

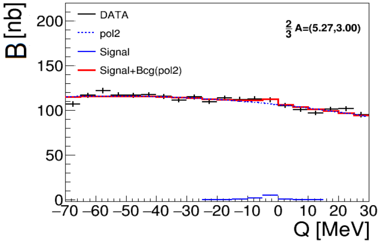

$$\sigma_{n\pi^0}(Q) = \frac{1}{3}A \cdot Theory(Q) + B_1 Q^2 + C_1 Q + D_1$$

$$\sigma_{p\pi^-}(Q) = \frac{2}{3}A \cdot Theory(Q) + B_2 Q^2 + C_2 Q + D_2$$

isospin relation between the both of the considered channels

$Theory(Q)$ - theoretical function after binning with the amplitude normalized to unity
$B_{1,2}Q^2 + C_{1,2}Q + D_{1,2}$ - polynomial of the second order

Fit performed for theoretical spectra obtained for different optical potential parameters (V_0, W_0)

Comparison with N. Ikeno et al. model prediction

results obtained for different optical potential parameters (V_0, W_0)

V_0	W_0	A (fit) [nb]	$\sigma_{upp}^{CL=90\%}$ [nb]
-30	-5	-5.0±3.9	6.5
-30	-20	-2.2±3.5	5.8
-30	-40	0.2±3.8	6.3
-50	-5	0.1±3.8	6.3
-50	-20	3.3±4.1	6.8
-50	-40	6.0±4.2	6.9
-70	-5	6.4±4.5	7.4
-70	-20	7.9±4.5	7.4
-70	-40	7.5±3.7	6.1
-100	-5	6.3±4.5	7.4
-100	-20	6.9±3.9	6.4
-100	-40	5.3±3.1	5.2

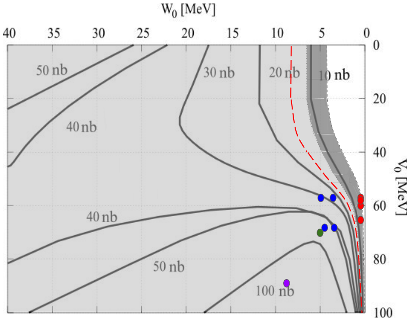

Contour plot of the theoretically determined conversion cross section in $V_0 - W_0$ plane.

The allowed parameter space ($|V_0| <\sim 60$ MeV and $|W_0| <\sim 7$ MeV) excludes most optical model predictions of $\eta-^{4}$He nuclei except for some loosely bound narrow states.

M. Skurzok, P. Moskal, et al., Phys. Lett. B 708, 6 (2018)

Search for $(^3He\text{-}\eta)_{bound}$ with WASA-at-COSY

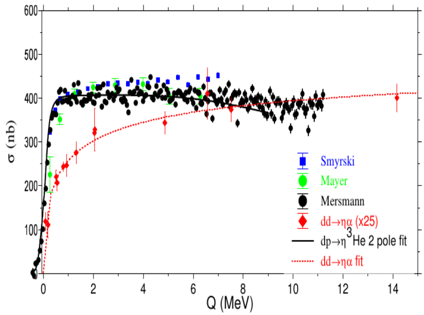

$$\sigma_{pd\to^3He-\eta} \approx 25\sigma_{dd\to^4He-\eta}$$

About 2 weeks of measurement allowed us to reach sensitivity of **few nb** $(L \approx 4500\frac{1}{nb})$

Measurement: p_{beam} : 1.468-1.615GeV/c, **Q∈(-70,30)MeV**

Channels:

- **Via the resonance decay N^*:**
  1) $pd \to (^3\text{He-}\eta)_{bound} \to ppp\pi^-$
  2) $pd \to (^3\text{He-}\eta)_{bound} \to ppn\pi^0$
  3) $pd \to (^3\text{He-}\eta)_{bound} \to dp\pi^0$

  Aleksander Khreptak PhD

- **Absorption of orbiting η**
  4) $pd \to (^3\text{He-}\eta)_{bound} \to {}^3\text{He}\ 2\gamma$
  5) $pd \to (^3\text{He-}\eta)_{bound} \to {}^3\text{He}\ 6\gamma$

  Oleksandr Rundel PhD

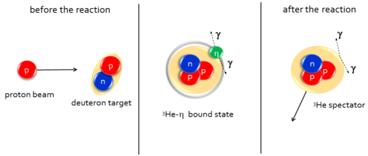

$pd \rightarrow (^3\text{He-}\eta)_{bound} \rightarrow dp\pi^0$ analysis

Simulations

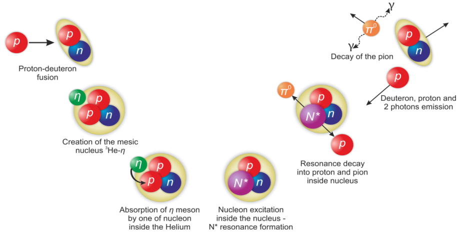

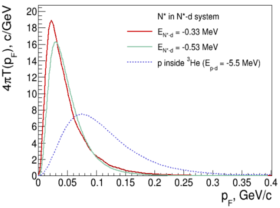

N. Kelkar et al., Int. J. Mod. Phys. E 28, 1950066 (2019);
N. Kelkar et al., Nucl. Phys. A 996, 121698 (2020)

Events selection

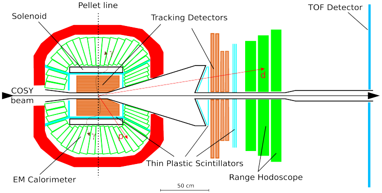

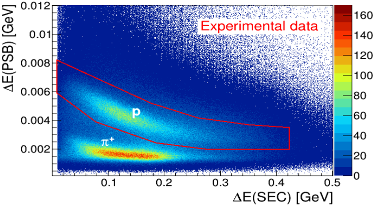

Upper limit of the total cross section

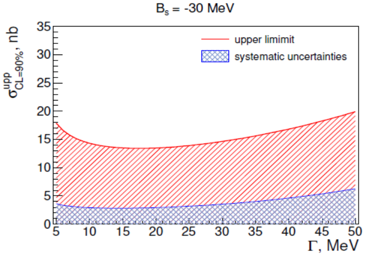

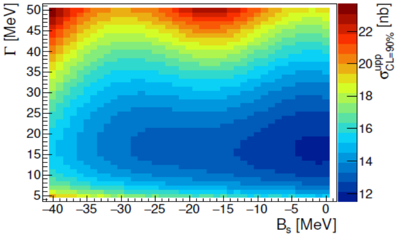

Result

$$13\ nb \leq \sigma^{upp}_{pd\rightarrow(^3\text{He-}\eta)_{bound}\rightarrow dp\pi^0} \leq 24\ nb$$

P. Adlarson et al., Phys. Rev. C 102, 044322 (2020)

Previous result:

COSY-11 $\sigma_{pd\rightarrow(^3He-\eta)_{bound}\rightarrow ^3He\pi^0} < 70\ nb$

J. Smyrski et al., Nucl. Phys. A 790 (2007) 438

Simulation of $pd \rightarrow (^3\text{He-}\eta)_{bound} \rightarrow {}^3\text{He}\ 2\gamma(6\gamma)$

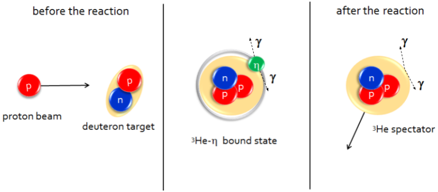

- **^{3}He is spectator $|\mathbb{P}_{^3He}|^2 = m^2_{^3He}$**
- **Fermi momentum distribution of the η meson in ^{3}He-η bound system**

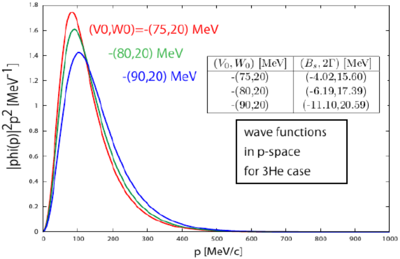

- **bound η decays to 2γ or $3\pi^0$**

M. Skurzok et al., Nucl. Phys. A 993, 121647 (2020)

Structure of hypothetical ^{3}He-η bound state can be described as a solution of Klein-Gordon equation:

$$\left[-\vec{\nabla}^2 + \mu^2 + 2\mu U_{opt}(r)\right]\psi(\vec{r}) = E^2_{KG}\psi(\vec{r})$$

where: E_{KG} - Klein -Gordon energy, μ - ^{3}He-η reduced mass

optical potential:

$$U_{opt}(r) = (V_0 + iW0)\frac{\rho(r)}{\rho_0}$$

where: $\rho(r)$ - density distr. for ^{3}He, ρ_0 - normal nuclear density

KG equation solved for several sets of (V_0, W_0)

$$\Downarrow$$

$$E_{KG},\ \psi(\vec{r})$$

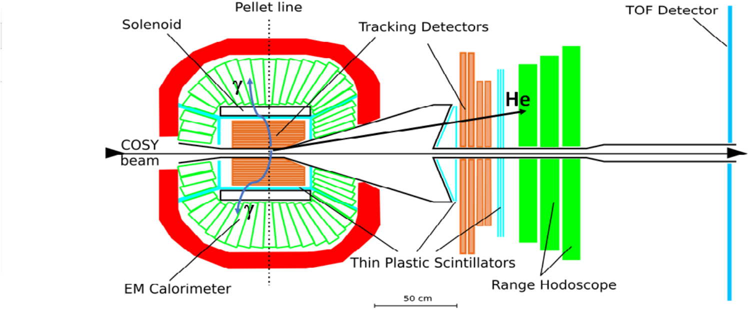
Pellet line
Solenoid
Tracking Detectors
TOF Detector
He
COSY beam
Thin Plastic Scintillators
Range Hodoscope
EM Calorimeter
50 cm

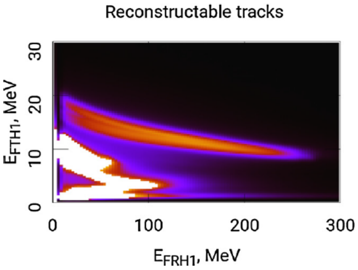
Reconstructable tracks
E_{FTH1}, MeV
E_{FRH1}, MeV
0
10
20
30
0
100
200
300

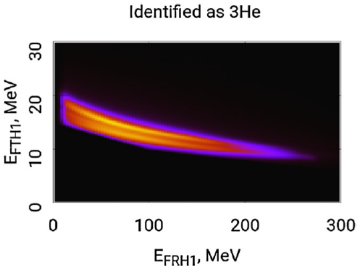
Identified as 3He
E_{FTH1}, MeV
E_{FRH1}, MeV
0
10
20
30
0
100
200
300

Events selection - $pd \to (^3\text{He-}\eta)_{bound} \to {}^3\text{He}\ 2\gamma$

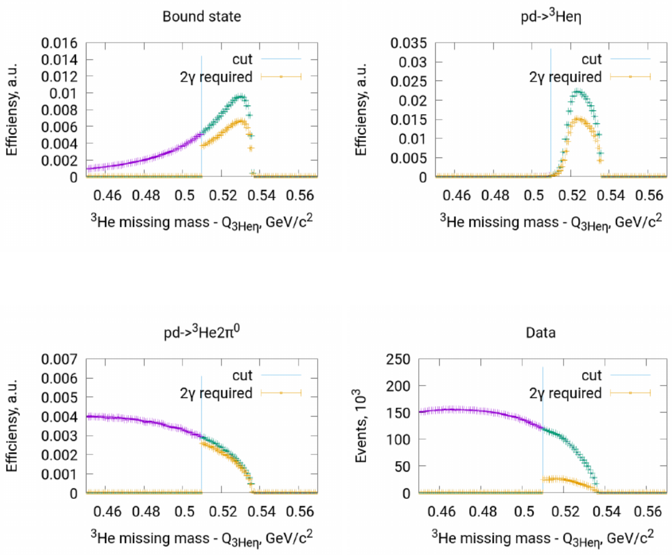

Excitation function $pd \to (^3\text{He-}\eta)_{bound} \to {}^3\text{He}\ 2\gamma$

Cross section

$$\sigma(Q) = \frac{N(Q)}{L(Q)\epsilon(Q)}$$

N - number of experimental events

L - integrated luminosity

ϵ - full detection efficiency

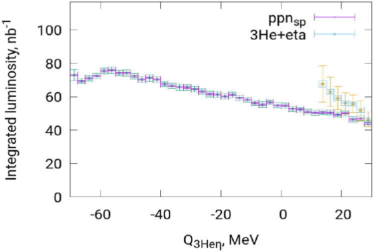

pd->^{3}He2γ

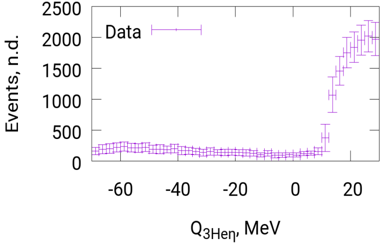

pd->^{3}He2γ

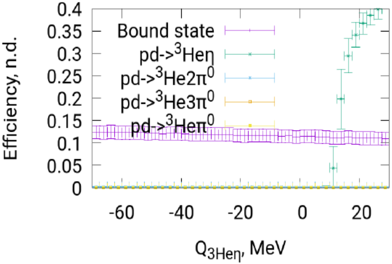

Excitation function $pd \to (^3\text{He-}\eta)_{bound} \to {}^3\text{He}\ 6\gamma$

Cross section

$$\sigma(Q) = \frac{N(Q)}{L(Q)\epsilon(Q)}$$

N - number of experimental events

L - integrated luminosity

ϵ - full detection efficiency

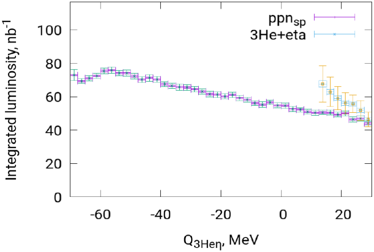

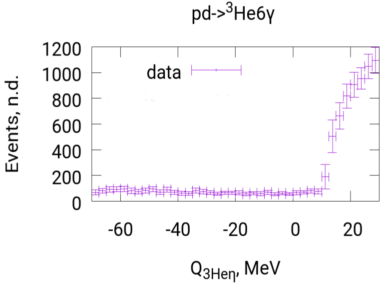

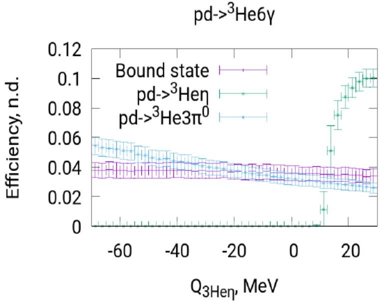

Determination of the upper limit of the total cross section for $pd \rightarrow ({}^3\text{He-}\eta)_{bound} \rightarrow {}^3\text{He}2\gamma(6\gamma)$ processes at CL=90%

$pd \rightarrow ({}^3\text{He-}\eta)_{bound} \rightarrow {}^3\text{He}2\gamma$

$\Downarrow$

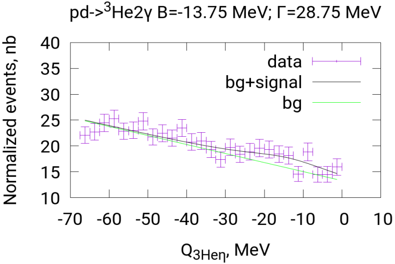

$pd \rightarrow ({}^3\text{He-}\eta)_{bound} \rightarrow {}^3\text{He}6\gamma$

$\Downarrow$

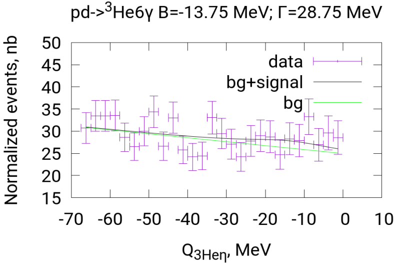

simultaneous fit with $P_{\eta decay}\frac{A\cdot\Gamma^2/4}{(Q-B_s)^2+\Gamma^2/4} + BQ + C$

Breit-Wigner (signal) + pol2 (background)

where $P_{\eta decay}$ are branching ratios for η decays:
$P_{\eta\rightarrow 2\gamma}=0.3941,\ P_{\eta\rightarrow 3\pi^0}=0.3268$

B_s,Γ - fixed parameters | A, B, C - free parameters || $\sigma^{upp}_{CL=90\%} = A + k\cdot\sigma_A$, k=1.64 (for CL=90%)

Determination of the upper limit of the total cross section for $pd \to (^3\text{He-}\eta)_{bound} \to {}^3\text{He}2\gamma(6\gamma)$ process at CL=90%

$\sigma^{upp}_{CL=90\%}$ for

$pd \to (^3\text{He-}\eta)_{bound} \to {}^3\text{He}2\gamma(6\gamma)$

$\Downarrow$

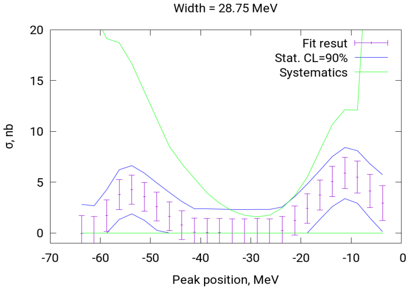

RESULT:

$\sigma_{pd\to(^3He-\eta)_{bound}\to^3He2\gamma(6\gamma)} < 15\ nb$

INDICATION:-)

slight indication of the signal from the bound state for $\Gamma > 20$ MeV and $B_s \in (0, 15)$ MeV

$(100 < V_0 < 70 MeV$ and $|W_0| > 20 MeV) \Downarrow$

However, the observed indication is within the range of the systematic error

$\Downarrow$

we cannot make a definite conclusion here on possible bound state formation

Previous result:

COSY-11

$\sigma_{pd\to(^3He-\eta)_{bound}\to^3He\pi^0} < 70\ nb$

J. Smyrski et al., Nucl. Phys. A 790 (2007) 438

P. Adlarson et al., Phys. Lett. B 802, 135205 (2020)

Summary of the search for η-mesic Helium at WASA

$(^4\text{He-}\eta)_{bound}$

- **2008**: $dd \to {}^3\text{He}p\pi^-$ reaction

$$\sigma_{dd\to(^4He-\eta)_{bound}\to{}^3Hep\pi^-} < 27\ nb$$

- **2010**: $dd \to {}^3\text{He}n\pi^0$ and $dd \to {}^3\text{He}p\pi^-$ reactions

$$\sigma_{dd\to(^4He-\eta)_{bound}\to{}^3Hep\pi^-} < 7\ nb$$

$$\sigma_{dd\to(^4He-\eta)_{bound}\to{}^3Hen\pi^0} < 3.5\ nb$$

$(^3\text{He-}\eta)_{bound}$

- **2014**: $pd \to {}^3\text{He}2\gamma$ and $pd \to {}^3\text{He}6\gamma$ reactions

$$\sigma_{pd\to(^3He-\eta)_{bound}\to{}^3He2\gamma(6\gamma)} < 15\ nb$$

- **2014**: $pd \to dp\pi^0$ reaction

$$\sigma_{pd\to(^3He-\eta)_{bound}\to dp\pi^0} < 24\ nb$$

Summary and Conclusions

- Search for η-mesic helium was carried out using the ramped beam technique.
- No bound state signal visible in 2008 data (upper limit of the total cross section for the bound state production determined)
- 2010 measurement doesn't show a narrow signal of η-mesic nuclei in $dd \rightarrow {}^3\mathrm{He}n\pi^0$ and $dd \rightarrow {}^3\mathrm{He}p\pi^-$ channels
- 2014 measurement doesn't show a narrow signal of η-mesic nuclei in $pd \rightarrow {}^3\mathrm{He}2\gamma$, $pd \rightarrow {}^3\mathrm{He}6\gamma$ and $pd \rightarrow dp\pi^0$ channels
- The upper limits for $dd \rightarrow ({}^4\mathrm{He}\text{-}\eta)_{bound} \rightarrow {}^3\mathrm{He}p\pi^-$ and $dd \rightarrow ({}^4\mathrm{He}\text{-}\eta)_{bound} \rightarrow {}^3\mathrm{He}n\pi^0$reaction in order of **few nb**!
- The upper limits for $pd \rightarrow {}^3\mathrm{He}2\gamma(6\gamma)$ reactions $<$ **15 nb**!
- The upper limit for $pd \rightarrow dp\pi^0$ reactions $<$ **24 nb**!

Thank you for attention

Selection criteria

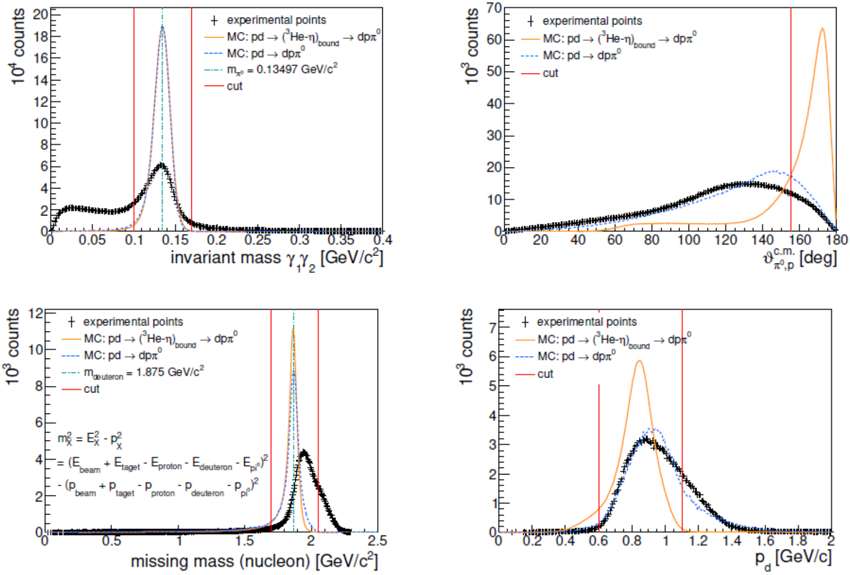

Determination of the excitation function

Excitation function

$$\sigma(Q) = \frac{N(Q)}{\varepsilon(Q) \cdot L(Q)}$$

N – number of experimental events

ε – reconstruction efficiency

L – integrated luminosity

Number of events

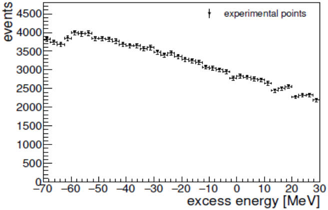

Efficiency

$pd \rightarrow (^3\text{He-}\eta)_{bound} \rightarrow dp\pi^0$

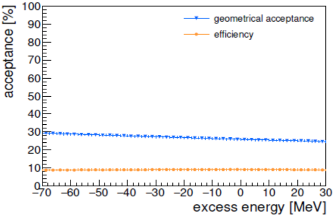

Integrated luminosity

$pd \rightarrow ppn_{spectator}$

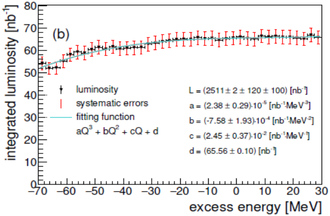

Upper limit of the total cross section

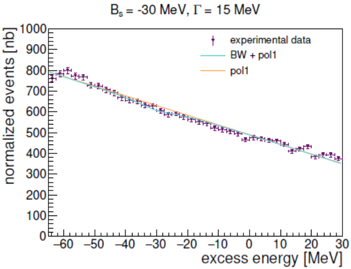

Fit with a Breit–Wigner function combined with a first order polynomial:

$$\frac{A \cdot \frac{\Gamma^2}{4}}{(Q - B_s)^2 + \frac{\Gamma^2}{4}} + BQ + C$$

Breit-Wigner (signal) + pol1 (background)

B_s and Γ are fixed parameters; A, B, C are free parameters.

$$\sigma^{upp}_{CL=90\%} = k \cdot \sigma_A, \; k = 1.64 \; (CL = 90\%)$$

Events selection - $pd \to (^3\text{He-}\eta)_{bound} \to {}^3\text{He}\ 2\gamma$

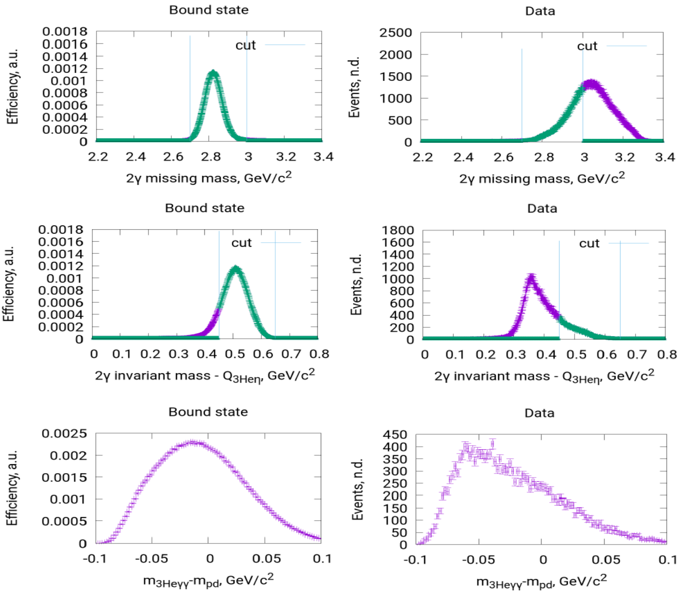

Forschungszentrum Jülich, Germany

COoler SYnchrotron COSY

Motivation

- Search for new kind of nuclear matter
- Investigation of η interaction with nucleons inside a nuclear matter
- Information about η meson structure:
  the η meson binding inside nuclear matter is very sensitive to the singlet component (η-η' mixing) in the wave function of the η meson
  η-η' mixing $\Rightarrow$ binding increase
  S. D. Bass and P. Moskal, Rev. Mod. Phys. 91, 015003 (2019)
  S. D. Bass, A. W. Thomas, Phys. Lett. B634, 368 (2006)
  S. Hirenzaki, H. Nagahiro, Acta Phys. Polon. B45, 619 (2014)
- Study of N*(1535) properties in medium (probe of testing different N*(1535) models)
  S. Hirenzaki et al., Acta Phys. Polon. B41, 2211 (2010)
  D. Jido, H. Nagahiro, S. Hirenzaki, Phys. Rev. C66, 045202 (2002)
  Z.-W. Liu et al., Phys. Rev. Lett. 116, 082004 (2016)

Properties of η meson

mass	547.862 ± 0.017 MeV
width	1.31 ± 0.05 keV
$I^G(J^{PC})$	$0^+(0^{-+})$
η is an eigenstate to	P, C, G and CP
C $\vert\eta>$=+1 $\vert\eta>$	P $\vert\eta>$=-1 $\vert\eta>$
Decay modes	**Branching ratio**
Charged modes	28.10±0.34 %
$\eta \to \pi^+\pi^-\pi^0$	22.92±0.28 %
$\eta \to \pi^+\pi^-\gamma$	4.22±0.16 %
other modes	0.76 %
Neutral modes	72.912±0.34 %
$\eta \to 2\gamma$	39.41±0.20 %
$\eta \to 3\pi^0$	32.68±0.23 %
other modes	0.03 %

P. A. Zyla et al. (PDG), Prog. Theor. Exp. Phys. 2020, 083C01 (2020).

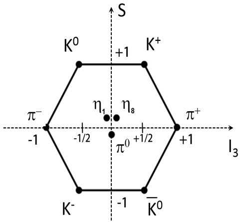

$$\eta_1 = \frac{1}{\sqrt{3}}(d\bar{d} + u\bar{u} + s\bar{s}),$$
$$\eta_8 = \frac{1}{\sqrt{6}}(d\bar{d} + u\bar{u} - 2s\bar{s}).$$

The observed η particle is the combination of the η_1 and η_8 states:

$|\eta> = \eta_8 cos\theta - \eta_1 sin\theta$, θ = -15.5°±1.3°

Hadronic decays (3π) (isospin breaking: $m_u - m_d$)

Radiative decays ($\gamma\gamma$ ($\pi\pi$))

(Semi-) leptonic decays (l l (γ))

$\eta \to e^+e^-\gamma$

$\eta \to e^+e^-e^+e^-$

Exp. indications of the existence of the ^{3}He-η bound state

total cross section $pd \to {}^3$He-η γ^3He $\to {}^3$He-η

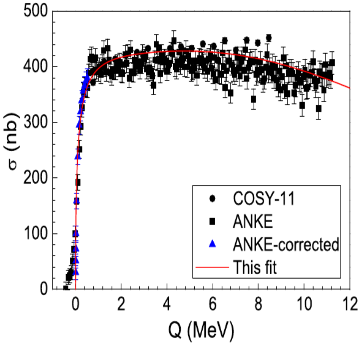

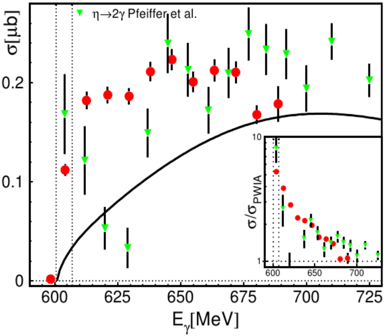

$\Downarrow$

J. Smyrski, et al., Phys. Lett. 649, 258 (2007)
T. Mersmann, et al., Phys. Rev. Lett. 98, 242301 (2007)
J.-J. Xie, et al., Phys. Rev. C 95, 015202 (2017)
B. Krusche, C. Wilkin, Prog. Part. Nucl. Phys. 80, 43 (2014)

Simulation of $pd \rightarrow (^3\text{He-}\eta)_{bound} \rightarrow dp\pi^0$

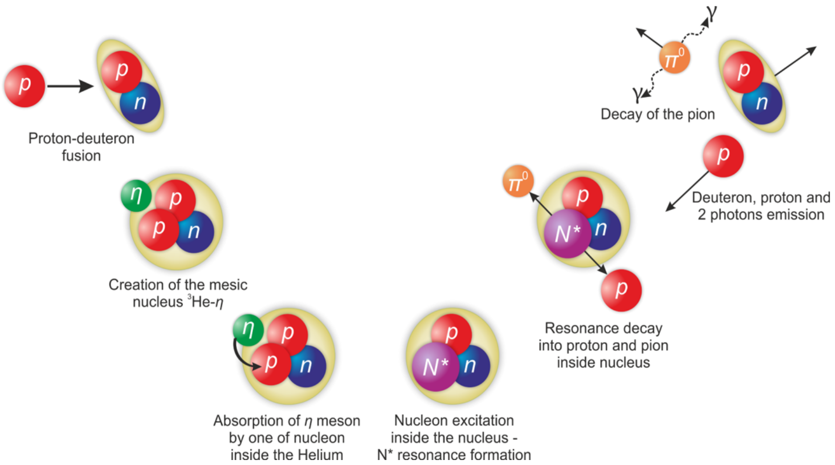

Simulation of $pd \rightarrow (^3\text{He-}\eta)_{bound} \rightarrow dp\pi^0$

Breit-Wigner distribution

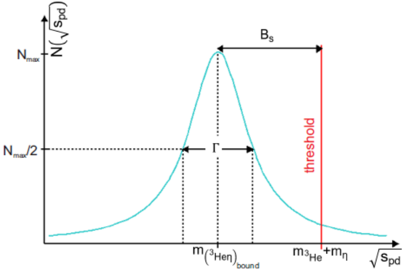

N* momentum distribution

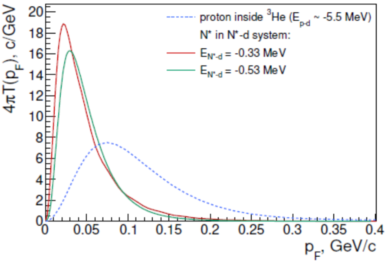

Breit-Wigner formula

$$N(\sqrt{s_{pd}}) = \frac{\Gamma^2/4}{\left(\sqrt{s_{pd}} - (m_\eta + m_{^3He} - B_s)\right)^2 + \Gamma^2/4}$$

$$B_s \in (0, 40)\ MeV; \Gamma \in (5, 50)\ MeV$$

N. Kelkar et al., Int. J. Mod. Phys. E 28, 1950066 (2019);
N. Kelkar et al., Nucl. Phys. A 996, 121698 (2020)

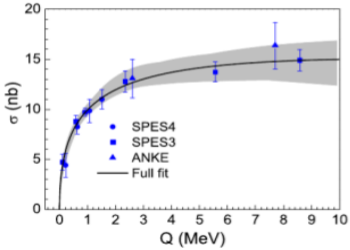

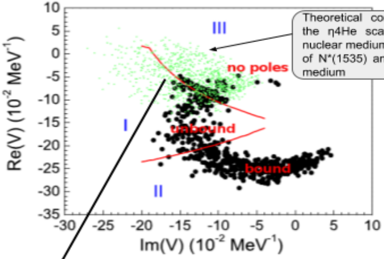

Theoretical constraints: model for the η4He scattering amplitude in nuclear medium based on excitation of N*(1535) and its modification in medium

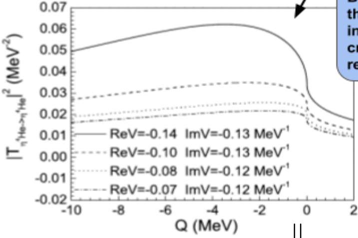

Bump structure below threshold related to the fast increase of the dd->4Heη cross section close to the reaction threshold

⇓

J.-J. Xie et al., Eur. Phys. J. A55 no.1, 6 (2019)

Analysis of $pd \rightarrow (^3He\text{-}\eta)_{bound} \rightarrow {}^3He\ 2\gamma$ process

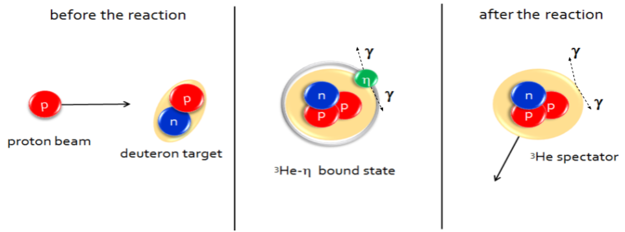

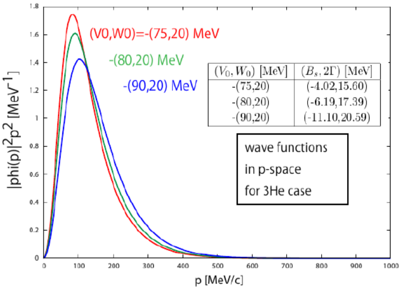

S. Hirenzaki, H. Nagahiro, Private communication (2016)

- ^{3}He spectator
- $P_{^3He} : p_{^3He} = \sqrt{m^2_{^3He} + p^2_{fermi}}$, distributed isotropically
- $P_{\eta_{bound}} = P_p + P_d - P_{^3He} \Rightarrow$
  $m_{\eta_{bound}} = |P_{\eta_{bound}}|$

Ikeno et al.

(V_0, W_0) [MeV]	(B_s, Γ_{abs}) [MeV]	$BR^*_{\eta\to 2\gamma}$	$BR^*_{\eta\to 3\pi^0}$
−(75,20)	(4.06, 15.66)	3.30×10^{-5}	2.73×10^{-5}
−(90,20)	(11.16, 20.65)	2.50×10^{-5}	2.07×10^{-5}
−(75,1)	(5.96, 0.76)	6.78×10^{-4}	5.62×10^{-4}
−(90,1)	(12.67, 1.02)	5.06×10^{-4}	4.20×10^{-4}

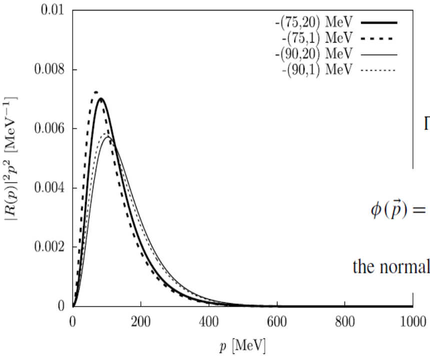

$$BR^*_{\eta\to 2\gamma/\eta\to 3\pi^0} = \frac{\Gamma_{\eta\to 2\gamma/\eta\to 3\pi^0}}{(\Gamma^{tot}_\eta + \Gamma_{abs})},$$

$$\Gamma_{\eta\to 2\gamma} = 0.3941 \times 1.31 \text{ keV} = 0.516 \text{ keV}$$

$$\Gamma_{\eta\to 3\pi^0} = 0.3268 \times 1.31 \text{ keV} = 0.428 \text{ keV}$$

$$\phi(\vec{p}) = \frac{1}{(2\pi)^{3/2}} \int e^{i\vec{p}\cdot\vec{r}} \psi(\vec{r}) d\vec{r},$$

the normalization condition $\int |R(p)|^2 p^2 dp = 1$

Events selection - $pd \to (^3\text{He-}\eta)_{bound} \to {}^3\text{He}\ 6\gamma$

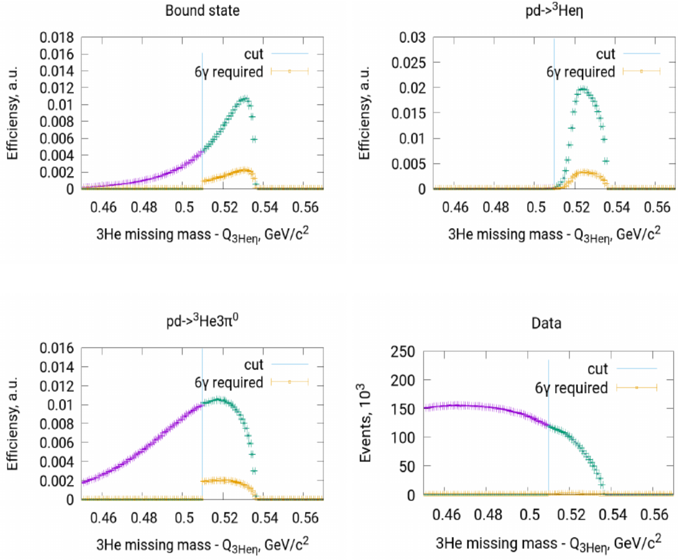

Events selection - $pd \to (^3\text{He-}\eta)_{bound} \to {}^3\text{He}\ 6\gamma$

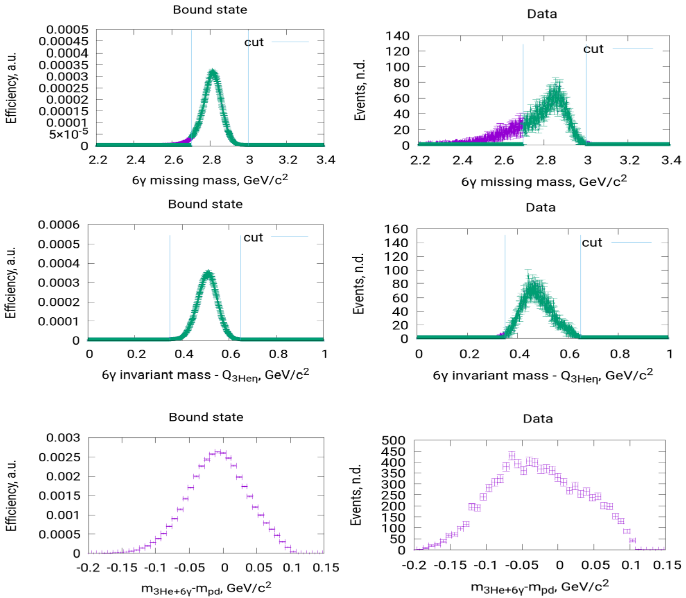

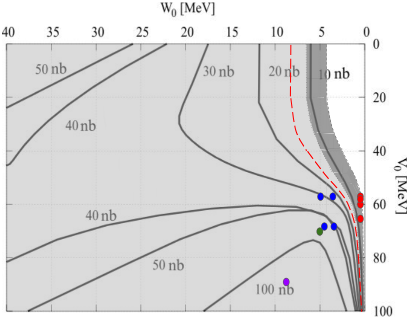

Purple and green - predictions based on the few body formalism with an optical model, where the complex η-nucleon scattering amplitude is obtained from (GW) a K-matrix description of the pN, ppN, ηN and γN coupled channels and fit to existing data (purple dot) and (CS) ηN amplitudes calculated within a chirally motivated separable potential model with the pa-rameters of the model fitted to N$\rightarrow$Nand N$\rightarrow$Ndata. (green dot).

N. Barnea, B. Bazak, E. Friedman, A. Gal, Phys. Lett. B, 771 (2017), 297

Blue- results obtained for a class of potentials including Gaussian, exponential and Hulthen (at E=0, l>0).

Red dots - predictions of very narrow and weakly bound states of 4He-η, with binding energies and widths in the range of ≈2–230 keV and ≈8–64 keV respectively, that are found by solving the Klein Gordon equation. These states correspond to the optical potential parameters $|V_0|$ in the range from 58 MeV to 65 MeV and $W_0 = 0.5$ MeV.